

# Evaluation of Garofalo Creep Model for Lead-free Solder Joints in Surface Mount Components

Emeka H. Amalu\*, N.N. Ekere\*, C. F. Oduoza\* and M. T. Zarmai\*

\*School of Engineering, Faculty of Science and Engineering,  
University of Wolverhampton,  
West Midlands, WV1 1LY, United Kingdom, E.Amalu@wlv.ac.uk

## ABSTRACT

This investigation employs four hyperbolic sine creep constitutive models to simulate the damage in Sn[3.0-4.0%]Ag[0.5-1.0%]Cu solder joints in flip chip (FC) model FC48 D6.3C457DC and resistor model R102 components assembled on printed circuit boards (PCBs). The creep models are proposed by Lau, 2003; Pang et al, 2003; Schubert et al, 2003 and Zang et al, 2003. The FC joints contain intermetallic compounds. All assemblies are subjected to accelerated high-temperature cycles utilising IEC Standard 60749-25 in parts. This study determines and compares the magnitude of accumulated creep strain and strain energy density generated from simulations using the various models and evaluates the effect of using the different creep relations to quantify damage and fatigue life of solder joints. The results show significant differences - demonstrating that predicted damage and fatigue life of solder joints depend on the value of creep parameters, damage index, creep model and geometry of solder joint.

**Keywords:** Constitutive creep model, lead-free solder, solder joint, creep damage, fatigue life.

## 1 INTRODUCTION

The adoption and use of different values of creep parameters proposed by numerous researchers in the Garofalo constitutive creep model has introduced significant variation in the predicted magnitude of damage and fatigue life of solder joints in electronic assemblies. The solder joints of surface mount components assembled on substrate printed circuit boards (PCBs) experience accelerated degradation which becomes critical when the assembly operates in high homologous temperature ambients. As the surface mount component assemblies are increasingly being used to assembly electronic devices deployed to control mission critical systems found in the aerospace, automotive, oil well-logging and medical devices, better understanding of the damage mechanics of their solder joints is crucial to predicting the assemblies mean-time-to-failure (MTTF),  $N_f$ . Accurate prediction has enormous benefits. It will inform on the right time for preventive maintenance and replacement of vulnerable component assembly. Such operations mitigate accidental system failure. If unprevented, system failure leads to loss of lives and properties.

## 2 CONSTITUTIVE MODELS, CREEP PARAMETER VALUES AND FATIGUE LIFE OF SnAgCu SOLDER

Many researches which include Lau 2003 [1], Pang et al 2004 [2], Schubert et al 2003 [3] and Zhang et al 2003 [4] have proposed parameter values for Garofalo constitutive creep relation for lead-free solder joint. Table 1 presents these different values of creep parameters which have been used by many researchers to qualify and determine the magnitude of damage and fatigue life of solder joints in electronic assembly that is subjected to accelerated temperature cycles (ATCs).

The mathematical expressions for the constitutive relations  $E_1$  and  $E_2$  are:

$$E_1 : \dot{\varepsilon}_{ij}^{cr} = C_1 \left[ \sinh(C_2 \sigma_{eff}) \right]^{C_3} \exp\left(-\frac{C_4}{T}\right) \frac{3}{2} \frac{s_{ij}}{\sigma_{eff}} \quad (1)$$

$$E_2 : \dot{\varepsilon}_{cr} = C_1 \left[ \sinh(C_2 \sigma) \right]^{C_3} \exp\left(-\frac{C_4}{T}\right) \quad (2)$$

Where  $\dot{\varepsilon}_{ij}^{cr}$ ,  $\dot{\varepsilon}_{cr}$ ,  $\sigma$ , and  $T$  are the scalar creep strain rates, von Mises effective stress and absolute temperature, respectively. The other symbols represent material dependent parameters. The values of the parameters  $C_1$ ,  $C_2$ ,  $C_3$  and  $C_4$  are as presented in Table 1.

The mathematical models proposed by Syed [5] which relates solder fatigue lives  $N_{f(\varepsilon_{acc})}$  or  $N_{f(\omega_{acc})}$  to accumulated creep stain ( $\varepsilon_{acc}$ ) or strain energy density ( $\omega_{acc}$ ) in the joint are presented in Eqs. (3) and (4), respectively.

$$N_{f(\varepsilon_{acc})} = (0.0513 \times \varepsilon_{acc})^{-1} \quad (3)$$

$$N_{f(\omega_{acc})} = (0.00165 \times \omega_{acc})^{-1} \quad (4)$$

The values of  $\varepsilon_{acc}$  and  $\omega_{acc}$  are computed from outputs of computer simulation.

### 3 FINITE ELEMENT MODELING

The finite element modelling of the assemblies starts with geometric model creation. Three-dimensional (3D) geometric models of assembly of FC and Resistor components are created using both Ansys DesignModeler and SolidWorks software. The detailed architecture of the FC48 and R102 can be found in Toplevel dummy component catalogue and previous study [6]. The assemblies are presented in Figures 1 and 2 while Figures 3 and 4 depict solder joints of the various assemblies with default mesh.

The key materials in the assembly of the two components are presented in Tables 2 and 3. These tables also show the mechanical properties of the materials.

The two models shown in Figures 1 and 2 were subjected to six complete accelerated temperature cycles (ATCs) in 25 load steps. The plot of temperature profiles as a function of the time steps used in this investigation is presented in Figure 5. The temperature loading started from homologous temperature ( $T_H$ ) of 0.597, ramped up at the rate of 15 °C/min to excursion temperature (ET) of 0.86, where it dwelled for 10 minutes. It was then ramped down to  $T_H$  of 0.476 at the same rate, where it rested for 10 minutes. This magnitude of ramp rate is used because Aoki et. al. [7] reports that the internationally accepted ramp rate of 10 to 15 °C per minute is required by test standard IEC60749-25 temperature cycling (JESD22-A104-B), established for evaluating the reliability of semiconductor parts and assembly printed wire boards (PWBs). The assemblies are simply supported and some assumptions are made to simplify the structure for analysis.

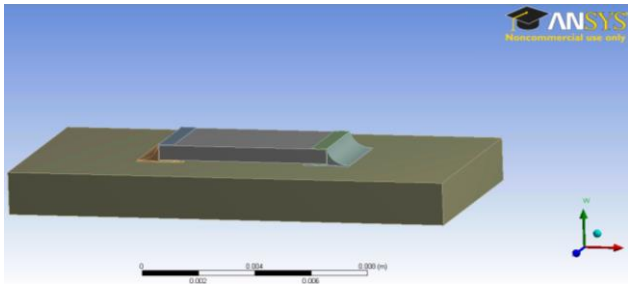


Figure 1: Assembly of resistor component on PCB.

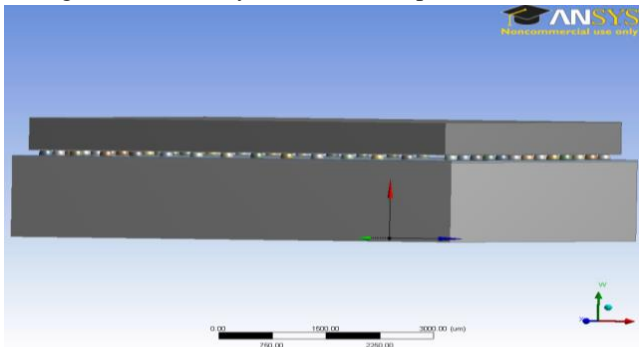


Figure 2: Assembly of flip chip component on PCB.

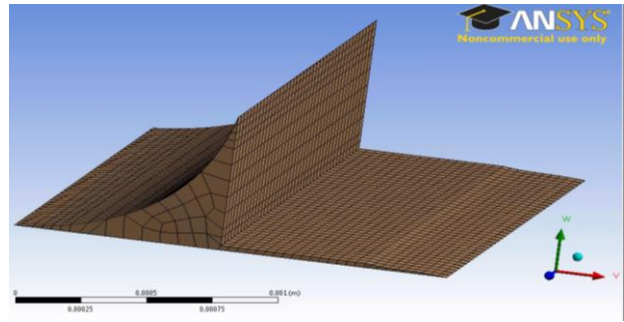


Figure 3: A solder joint of the resistors R102 assembly.

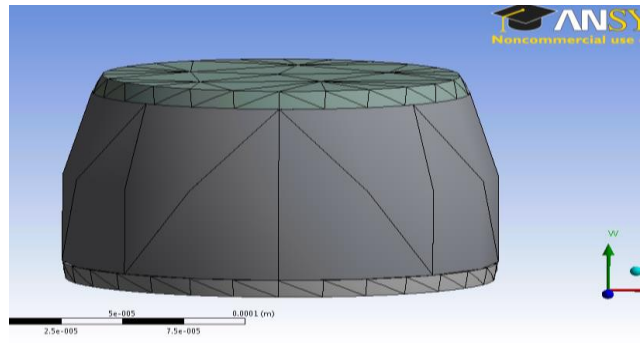


Figure 4: A solder joint of the flip chip FC48 assembly.

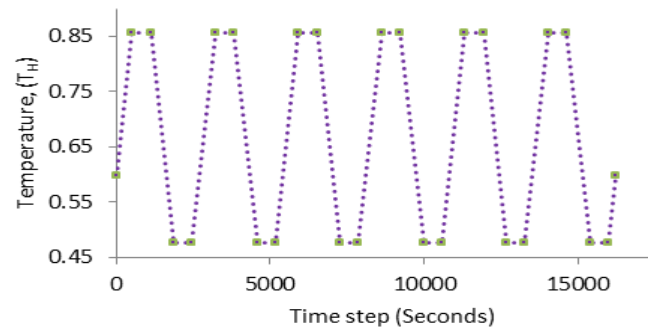


Figure 5: Plots of temperature cycles against time.

Table 1: Creep parameter values for Garofalo solder constitutive model

Model type	Proposer	Constitutive relation designation	Creep parameter values				Test vehicle	Solder composition
			$C_1$ ( $s^{-1}$ )	$C_2$ (MPa) $^{-1}$	$C_3$	$C_4$		
Hyperbolic sine law	Lau 2003	$E_1$	4.41E+05	0.005	4.2	5412	Not available	Not available
	Pang et al 2004	$E_2$	3.20E+04	0.037	5.1	6524.7	Machined from solder bar.	Sn3.8Ag0.7Cu
	Schubert et al 2003	$E_2$	2.78E+05	0.02447	6.41	6500	Data from different sources and casting	Sn3.8Ag0.7Cu, Sn3.5Ag0.75Cu, Sn3.5Ag0.5Cu.
	Zhang et al 2003	$E_2$	143.4	0.108	3.7884	7567	Single lap shear specimen	Sn3.9Ag0.6Cu

Table 2: Mechanical properties of materials in FC assembly

S/No	Component	Young's Modulus (GPa)			C.T.E (ppm/ $^{\circ}$ C)			Poisson Ratio			Shear Modulus (GPa)		
		$E_x$	$E_y$	$E_z$	$\alpha_x$	$\alpha_y$	$\alpha_z$	$\nu_{xy}$	$\nu_{xz}$	$\nu_{yz}$	$G_{xy}$	$G_{xz}$	$G_{yz}$
1	Die[8]	130.00			3.30			0.28			50.80		
2	Mask[9]	4.14			30.00			0.40			1.48		
3	Cu pad[10]	129.0			17.0			0.34			48.1		
4	Sn3.9Ag0.6Cu[11]	43.0			23.2			0.30			16.5		
5	Cu-Sn IMC[12]	110.0			23.0			0.30			42.3		
6	PCB[13]	27.0	27.0	22.0	14.0	14.0	15.0	0.17	0.2	0.17	27.0	22.0	27.0

Table 3: Mechanical properties of materials in resistor assembly

S/No	Component	Young's Modulus (GPa)			C.T.E (ppm/ $^{\circ}$ C)			Poisson Ratio			Shear Modulus (GPa)		
		$E_x$	$E_y$	$E_z$	$\alpha_x$	$\alpha_y$	$\alpha_z$	$\nu_{xy}$	$\nu_{xz}$	$\nu_{yz}$	$G_{xy}$	$G_{xz}$	$G_{yz}$
1	Resistor die (Alumina) [8]	282.7			6.0			0.2222			115.67		
2	Silver (Termination)[9]	83			18.9			0.37			30.29		
3	Copper pad[10]	129.0			17.0			0.34			48.1		
4	Sn3.9Ag0.6Cu solder[11]	43.0			23.2			0.30			16.5		
5	PCB [13]	27.0	27.0	22.0	14.0	14.0	15.0	0.17	0.2	0.17	27.0	22.0	27.0

## 4 RESULTS AND DISCUSSION

The damage experienced by solder joints may be analysed using  $\epsilon_{acc}$  and  $\omega_{acc}$ . The schematic of the damage distribution is presented in Figs. 6 and 8. They show that damage concentrates at the periphery of the joints which are potential site of crack initiation. These sites need to be strengthened to mitigate crack initiation and propagation. A study of Figures 7 and 9 reveals that each of the models produces creep damage profile that are similar in trend to the rest of the models but differ in magnitude.

The model proposed by Pang et al yields highest magnitude in the two assemblies. The model proposed by Lau and Zhang et al yield the least magnitudes in R102 and FC48 solder joints, respectively. In Figure 9, the magnitudes of equivalent creep strain predicted by Pang et al and Schubert et al are quite close. An investigation of effect of the various constitutive relations on the predicted value of  $\epsilon_{acc}$ ,  $\omega_{acc}$  and  $N_f$  are carried out. The results are presented in Table 4. It can be seen in the table that there are significant differences in the predicted values – demonstrating their dependence on creep parameter values.

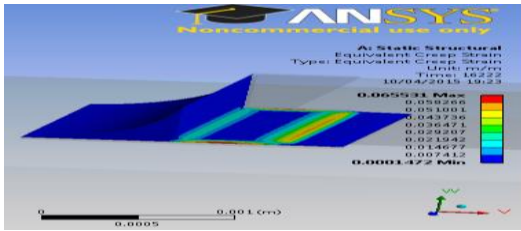


Fig 6: Equivalent creep strain damage in R102 solder joint.

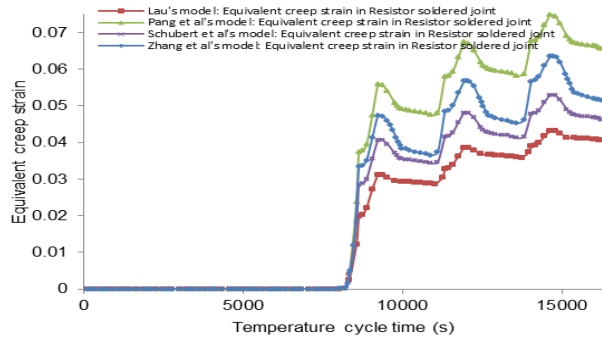


Fig 7: Plot of equi. creep strain vs temp. cycle time for R102.

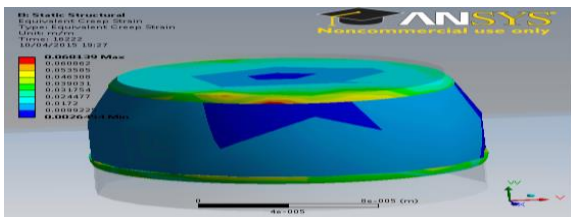


Fig 8: Equivalent creep strain damage in R102 solder joint.

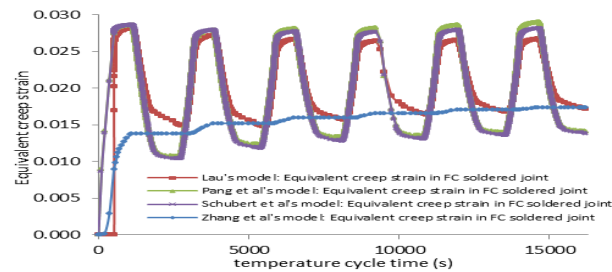


Fig 9: Plot of equi. creep strain vs temp. cycle time for FC48.

## 5 CONCLUSIONS

Based on the results of this investigation, it is difficult to identify which of the constitutive models predicts the damage and fatigue life of solder joint to the highest accuracy. However, it may be concluded that the magnitudes of these damage indices depend on the value of creep parameters used, damage index employed in the quantification, creep model utilised and the nature of geometry of solder joints investigated. The ball grid array geometry has demonstrated to be a better configuration than the resistor type solder joint and it is recommended to be used to assembly devices in mission critical systems. This observation calls for a review of all the existing models that may not have taken these findings into consideration and therefore suggests the development of new constitutive and life prediction models for accurate prediction of damage and fatigue life of solder joints in surface mount assemblies.

## REFERENCES

- [1] Lau, J.H. In *EPTC Conference*, Singapore, 2003.
- [2] Pang, J.H.L., et al, *ECTC*, Las Vegas, p.1333-1337, '04.
- [3] Schubert, A., et al. *ECTC*, New Orleans, p.603-610, 2003.
- [4] Zhang, Q. et al, *ECTC*, New Orleans, Louisiana, 2003.
- [5] Syed, A., *ECTC*, Las Vegas, Nevada, p. 737-746, 2004.
- [6] Amalu, E.H. et al, *J. of Mat. Proc. Tech.*, p.471-483, '12.
- [7] Aoki, Y. et al, *Espec Tech. Report*, No.25. p.4-13, 2007.
- [8] Zhang, Z., et al. *ECTC*, Las Vegas, Nevada, 2010.
- [9] Zahn, B.A. *ECTC*, San Diego, CA, 2002.
- [10] Nguyen, T.T., et al., *Microele. Relia.*, p.1000-1006, '10.
- [11] Stoyanov, S., C. et al., *S&S Mount Tech*, 2009, p. 11-24.
- [12] Sakuma, K., et al. *ECTC*, Las Vegas, Nevada, 2010.
- [13] *High Performance FR-4 for Multi-layered PWB Copper Clad Laminates*. 2009 17 Dec; Available from: [www.mgc.co.jp/eng/products/lm/btprint/lineup/fr4.html](http://www.mgc.co.jp/eng/products/lm/btprint/lineup/fr4.html).

Table 4: Predicted damage and life of solder joints in the assemblies using various constitutive models

Solder constitutive model	Accumulated creep strain		Accumulated creep strain energy density (MJ/m <sup>3</sup> )		Predicted life, N <sub>f</sub> (Cycle)			
					Based on accumulated creep strain		Based on accumulated creep strain energy density	
	FC48	R102	FC48	R102	N <sub>f(ε<sub>acc</sub>)</sub> (Syed 2004)	N <sub>f(ω<sub>acc</sub>)</sub> (Syed 2004)	N <sub>f(ε<sub>acc</sub>)</sub> (Syed 2004)	N <sub>f(ω<sub>acc</sub>)</sub> (Syed 2004)
Lau 2003	2.5E-03	4.1E-02	1.1E-04	5.8E-05	7892	481	5.6E+06	1.1E+07
Pang et al 2004	3.2E-03	6.6E-02	4.3E-05	2.8E-05	6130	298	1.4E+07	2.2E+07
Schubert et al 2003	3.4E-03	4.6E-02	8.6E-05	2.2E-05	5733	424	7.1E+06	2.8E+07
Zhang et al 2003	3.6E-03	5.1E-02	8.1E-04	3.9E-05	5483	382	7.5E+05	1.6E+07